JOURNAL OF
THE INTERNATIONAL ASSOCIATION
FOR SHELL AND SPATIAL
STRUCTURES

Prof. D. h-C Eng. E. TORROJA, founder

SPECIAL ISSUE

WG21 on:
ADVANCED MANUFACTURING AND MATERIAL

Guest Editor: **Arno PRONK**

Vol. 63 (2022) No. 2
June n. 212
ISSN: 1028-365X

Journal

VOL. 63 (2022) No. 2
n. 212 June

contents

WG21 on "Advanced Manufacturing and Material"

COVER: *Figure from paper by F. Laccone, L. Malomo, M. Callieri, T. Alderighi, A. Muntoni, F. Ponchio, N. Pietroni and P. Cignoni*

IASS Secretariat: CEDEX-Laboratorio Central de Estructuras y Materiales
Alfonso XII, 3; 28014 Madrid, Spain
Tel: 34 91 3357491; Fax: 34 91 3357422; https://iass-structures.org
journal@iass-structures.org; iass@iass-structures.org
Printed by SODEGRAF ISSN:1028-365X Depósito legal: M. 1444-1960

Vol. 63 (2022) No. 2 June n. 212

DESIGN AND CONSTRUCTION OF A BENDING-ACTIVE PLYWOOD STRUCTURE: THE FLEXMAPS PAVILION

Francesco LACCONE[1], Luigi MALOMO[2], Marco CALLIERI[3], Thomas ALDERIGHI[4], Alessandro MUNTONI[5], Federico PONCHIO[6], Nico PIETRONI[7] and Paolo CIGNONI[8]

[1]Postdoctoral Researcher, ISTI - CNR, Via Moruzzi 1, 56124 Pisa, Italy, francesco.laccone@isti.cnr.it
[2]Researcher, ISTI - CNR, Via Moruzzi 1, 56124 Pisa, Italy, luigi.malomo@isti.cnr.it
[3]Senior Researcher, ISTI - CNR, Via Moruzzi 1, 56124 Pisa, Italy, marco.callieri@isti.cnr.it
[4]PhD student, ISTI - CNR, Via Moruzzi 1, 56124 Pisa, Italy, thomas.alderighi@isti.cnr.it
[5]Technologist, ISTI - CNR, Via Moruzzi 1, 56124 Pisa, Italy, alessandro.muntoni@isti.cnr.it
[6]Researcher, ISTI - CNR, Via Moruzzi 1, 56124 Pisa, Italy, federico.ponchio@isti.cnr.it
[7]Senior Lecturer, University of Technology Sydney, 81 Broadway, Ultimo NSW, Australia, nico.pietroni@uts.edu.au
[8]Research Director, ISTI - CNR, Via Moruzzi 1, 56124 Pisa, Italy, paolo.cignoni@isti.cnr.it

Editor's Note: Manuscript submitted 15 December 2021; revision received 14 April 2022; accepted 15 June 2022. This paper is open for written discussion, which should be submitted to the IASS Secretariat no later than December 2022.

DOI: https://doi.org/10.20898/j.iass.2022.007

ABSTRACT

Mesostructured patterns are a modern and efficient concept based on designing the geometry of structural material at the meso-scale to achieve desired mechanical performances. In the context of bending-active structures, such a concept can be used to control the flexibility of the panels forming a surface without changing the constituting material. These panels undergo a formation process of deformation by bending, and application of internal restraints. This paper describes a new constructional system, FlexMaps, that has initiated the adoption of bending-active mesostructures at the architectural scale. Here, these modules are in the form of four-arms spirals made of CNC-milled plywood and are designed to reach the desired target shape once assembled. All phases from the conceptual design to the fabrication are seamlessly linked within an automated workflow. To illustrate the potential of the system, the paper discusses the results of a demonstrator project entitled FlexMaps Pavilion (3.90x3.96x3.25 meters) that has been exhibited at the IASS Symposium in 2019 and more recently at the 2021 17th International Architecture Exhibition, La Biennale di Venezia. The structural response is investigated through a detailed structural analysis, and the long-term behavior is assessed through a photogrammetric survey.

Keywords: *Bending-Active Structures, Computer Aided Design, Optimization, Shell Structures, Timber Spatial Structures, Structural Design*

1. INTRODUCTION

In all manufacturing fields, a large transition is taking place from the philosophy of mass production and modularity to the extreme customization of products. This transition is supported by an expanded availability of new computational tools and by the possibilities introduced by numerically-controlled machines, like cutters and material extruders. Research and practice in the architectural and structural fields are also moving in this direction. In such cases, the customization can be oriented towards aesthetics, shape requirements, mechanical performance (i.e. high strength or stiffness), and accomplishment of sustainability goals (i.e. material reduction or reuse) [1-9].

Based on these premises, workflows that seamlessly link design with physical production have become necessary to combine the multiple goals and constraints in a closed optimization loop. In particular, new techniques have been introduced for reinterpreting or abstracting the objects in a new style [10], preserving their shape or desired functions.

Mesostructures are man-made structures that can be regarded as an abstraction of continuous bodies. They are designed at the meso-scale in order to achieve a desired mechanical performance [11].

Figure 1: *The FlexMaps Pavilion at the Competition and exhibition of innovative lightweight structures, Form and Force, joint international conference of IASS Symposium 2019 and Structural Membranes 2019, and at the 2021 17th International Architecture Exhibition, La Biennale di Venezia*

The macroscopic behavior of these structures is mainly determined by the arrangement of the solid material rather than their micro-scale chemical matrix. Surface mesostructures that can be bent and stretched to deform into a pre-described shape can be used to form the skin of an object. In this case, the stiffness of each part is to be designed with respect to the target shape objective and to form a consistent structural assembly as a whole, i.e. stable, resistant and stiff.

This mechanical formation process of deforming a body and constraining it to form a certain shape is shared with the bending-active structures. Actively bending is an approach to build curved architectural surfaces made of flat, linear or planar, elements, which are designed to support an internal pre-stress derived from an imposed curvature during the assembly process [12-18]. Boundary constraints and internal joints lock the position of the elements once the desired spatial configuration is reached.

The form-finding of bending-active structures requires geometry- and physically-based methods to predict the deformation and the material stress at each stage of the formation process [19]. However, due to the complexity of this problem, only a few methods are sufficiently generic to allow imposing a target shape and finding the best arrangement of bending-active components to approximate it [20-22].

This paper reports on the knowledge acquired from the design, analysis, and construction of a bending-active structure entitled FlexMaps Pavilion, which is based on the computational framework of [23]. This prototype is shaped as a thin twisted strip composed of actively-bent patches. These patches embed carved spiral patterns made of plywood that serve as mesostructure.

The prototype has been created specifically for the "Competition and exhibition of innovative lightweight structures" organized in 2019 by the IASS Working Group 21 "Advanced manufacturing and materials" [24]. After this successful installation at the IASS, in which it was awarded the First Prize, it was selected to be exhibited within the Italian Pavilion of the 2021 17th International Architecture Exhibition, La Biennale di Venezia from May 22 to November 21, 2021 (Fig. 1). This venue has required a deeper understanding of the structure's long-term behavior and the elaboration of a monitoring plan to assess the safety level during the exhibition.

The structure design and construction are based on the following automated steps:

(i) the computational design, which outputs the decomposition of the shape into flat fabricable patches and computes the spiral patterns;

(ii) the detailed structural analysis;

(iii) the fabrication through CNC milling machines and the generation of the instructions for the assembly and monitoring;

(iv) the monitoring of the shape by means of photogrammetry survey.

Leveraging the lesson learned from the IASS 2019 experience, the analysis of the FlexMaps Pavilion has been revisited considering the requests of the 2021 Venice Biennale exhibition, in which the structure performs as a freestanding indoor installation and is located on a stiff basement provided by the host. The whole assembly composed by the structure and the basement is simply laid on the floor.

2. MATERIALS AND METHODS

A unique workflow links all the main design and construction steps to deliver the FlexMaps Pavilion, as shown in Fig. 2. This method is based on tiling and segmentation, so it starts from a continuous target shape and handles discrete units as four-arms spirals, which aim to approximate it.

The target shape constitutes the main input and can be obtained with any form-finding technique or be generic, i.e. conceived with a sculptural approach. As a lattice structure, the primary requirement for the shape is to be stable. From a theoretical point of view, there are no other restrictions on the shape, i.e. on the topology, Gaussian curvature, supports location. But practically, since the spirals form a discrete system, their size influences the capacity to approximate folds and sharp features, which cannot be included without expecting a large shape deviation. Additionally, the material can only attain a limited strength, so the spirals cannot be bent beyond the material capacity without breaking them. Thus, curvature beyond the material capacity is not allowed. The target shape of the FlexMaps Pavilion is a non-developable twisted strip with a variable curvature from point to point, which has been sculpturally designed to challenge the IASS 2019 competition requirements of fitting a maximum volume of 4.00 x 4.00 x 4.00 meters.

Other preliminary information and actions are required to initiate the computational design, such as the mechanical characterization of the constituent material and the fabrication setup knowledge (machine operations and tolerances).

The core process of the workflow lies in the computational design, in which the optimal mesostructure decomposition is found. Essentially, an inverse design problem is solved: given a continuous target shape and a set of geometrical and mechanical parameters, find of a set of spiral patches that once bent and assembled result as close as possible to the target shape if submitted to a given

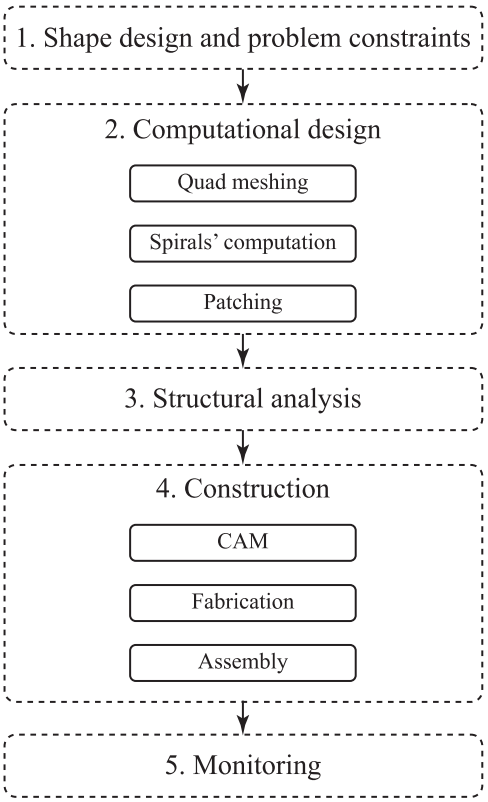

Figure 2: *Design workflow of FlexMaps structures*

load. The underlying idea is that the longer the spiral arms the softer is its mechanical response and the easier is to bend it/deform it. The general framework behind this process has been extensively described and investigated in [23], and it is recalled in Sec. 3 discussing the input values used for the specific application of the FlexMaps Pavilion.

A detailed structural analysis is performed to assess the safety level under the requirements of the Biennale exhibition. The model is automatically built from the output of the previous step and is made of 3D brick finite elements with orthotropic material properties. The results are included and discussed in Sec. 4.

The construction of the demonstrator builds directly on the output of the computational design step as well. All the elements to be fabricated are elaborated as a CAM for CNC milling machines. Handling the flat fabricated elements is sufficiently easy, while the most difficult step of the work is the assembly (and disassembly) because being a manual process requires experience. Several undesired failures may happen.

The assembly is designed to be carried out without shape control, so that the accuracy of the final shape solely relies on the self-formation capacity of the

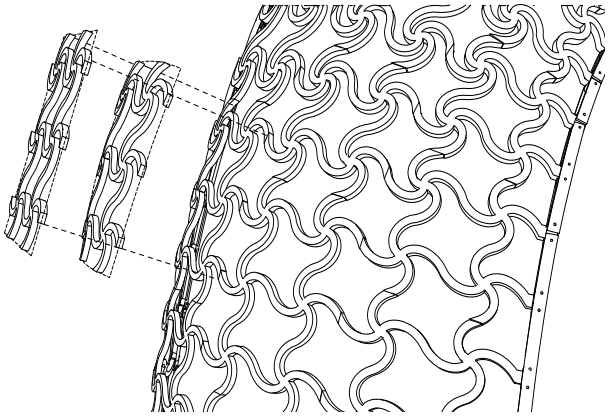

***Figure 3**: FlexMaps system description: the patches are fabricated as flat elements, then bent and assembled.*

structure. The photogrammetry survey is used to prove this accuracy, and it is later adopted to monitor the long-term displacements of the structure submitted to the exhibition conditions, i.e. constant load in humid environment.

2.1. System features

FlexMaps structures are thin mesostructured surfaces that can have free-form geometry. These surfaces are patterned with spirals, which are aligned on a grid so that one spiral is inscribed in a quad element of the grid. Although they form a 3D configuration, the spirals are fabricated from flat material sheets and then actively bent and mutually connected (Fig. 3).

The spirals define not only the unique aesthetics of the shell but also the proper load-bearing system. Each spiral is computationally designed through a bespoke algorithm that modifies its geometrical features without changing the constituent material, such that, once bent and connected to the neighboring ones, it assumes a predeterminate configuration under permanent load.

In the case of the FlexMaps Pavilion the spirals have approximately an equal size of about 0.25 x 0.25 m, but different twist (i.e. spin of the arms around their center). This is equivalent of having different tiles with a custom stiffness, and then characterized by differentiated attitude in bending. The bending is a self-formation process and introduces a state of pre-stress on the material.

For both shape accuracy and fabrication feasibility, the whole surface is required to be segmented. Thus, each patch is a fabricable module that is obtained out of flat material.

2.2. Detailed design

The structure is entirely made of Okumé plywood, which is CNC milled in shop from sheets of 20 mm thickness. The structure is a single-layer piecewise twisted shell that fits a bounding box of 3.90 x 3.96 x 3.25 meters. This non-trivial shape is non-developable, so it cannot be assembled as a single flat piece and then deformed, but it needs to be decomposed into several smaller developable flat patches. The Gaussian curvature of the shape is highly variable from positive values, close to the supports, to negative values in the central part, where the twisting takes place.

Spiral-to-spiral joints are located along the seams of the patches and are produced as key connectors, shown in Fig. 4 (a). These connectors are placed on the endpoints of spiral arms and are carved to have an interlocking shape that restrains any relative movement between the parts once assembled. Additionally, this interlocking shape is secured by two M5 bolts, coupled with large washers and installed on precision-drilled holes, which are located at the interface of the shape. The bolts thus enhance the shear and bending strength of the connection and guarantee its full-strength. The width of the material has been slightly enlarged to exactly compensate for the weakening introduced by seam. Indeed, it is crucial not to alter the overall stiffness of the structure by introducing weak or rigid spots.

To restrain the free boundaries of the structure, edge beams are provided, as in Fig. 4 (b). These devices consist of a couple of 8 mm lamellae that clamp the boundary connector by means of two bolts. These lamellae are designed as developable strips, which are fabricated as flat pieces and then actively bent during the assembly.

To secure the structure to the supports, the spiral arms on the lower boundary lines are in-plane shaped as T profiles. These are inserted within ground beams made of three plies of 20 mm plywood, as shown in Fig. 4 (c). The two lower plies restrain the in-plane position of the T connector, the upper ply locks the T and avoids the uplift.

Originally at the IASS exhibition, the two ground beams were mutually connected uniquely through a plywood paving with the role of balancing the thrust and twisting forces. This paving is made of variable-density Voronoi tiles with a decreasing size from the supports to the center. The edges of the Voronoi polygons are dry interlocking (Fig. 5) and the paving

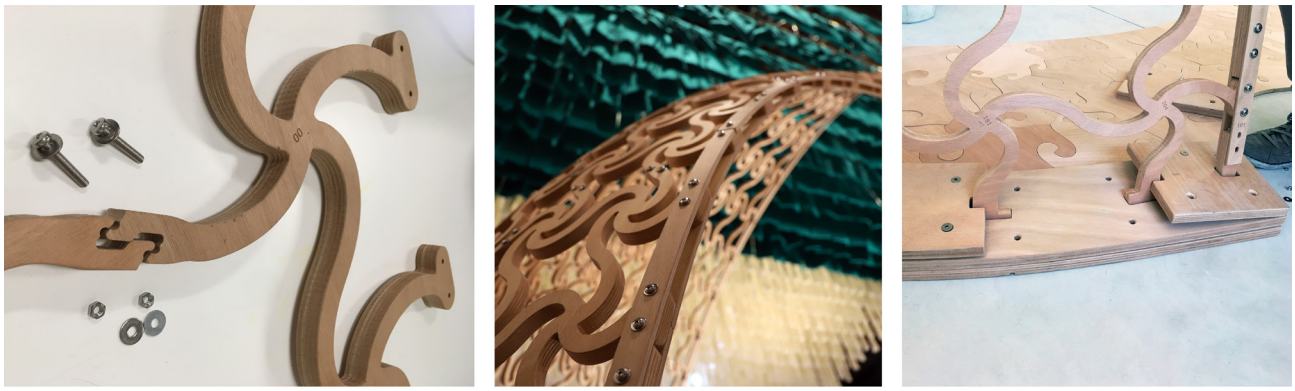

(a) *(b)* *(c)*

***Figure 4**: Detailed design of FlexMaps system: (a) patch-to-patch joint; (b) free boundaries joint; (c) supports joint*

is linked to the ground beams by means of dovetail joints. At the Biennale, due to the increased exhibition time span, the stiffness of these supports is increased for the sake of safety, so the ground beams are rigidly fixed on a supporting platform. However, the paving has been kept as an additional safety measure and for aesthetic reasons. The assembly composed by the structure and the supporting platform constitutes a self-equilibrated unit, which is simply laid on the existing paving. The adopted structural cross sections are:

- 20 x 20 mm for the spiral panels;
- two lamellae of 20 x 8 mm for the edge beams;
- three plies of 200 x 20 mm for the ground beams;
- 12-mm-thick paving tiles.

2.3. Materials

The plywood material adopted in this work is for both general purpose use (non-structural application) and structural applications in dry, humid, or exterior conditions (EN 636:2012). To comply with the environmental conditions of the exhibition, a Service Class 2 is adopted as per EN 1995-1-1 (use in humid conditions). The material is Okumé plywood, whose performances as declared by the manufacturer are included in Tab. 1.

***Table 1:** Material parameters deduced from the manufacturer technical data*

Thickness (mm)	Service Class	Strength	Young's modulus
20 mm	Class 3	42 N/mm^2	4200 N/mm^2

The material is classified Bending strength class F25 and Modulus of elasticity in bending class E40 (EN 636:2012+A1:2015) in both the directions of the grain and perpendicular to the grain of the outer layer of plywood. The characteristic values of the mechanical properties are derived by cross-referencing with EN 12369-2.

***Figure 5:** Variable-density interlocking Voronoi paving tiles.*

The density of $\rho_{w,mean} = 500\ kg/m^3$ is determined according to EN 323. The strength properties are computed as $X_d = k_{mod}\, X_k/\gamma_M$, in which X is the generic mechanical parameter, $k_{mod} = 0.6$ for permanent loads, and $\gamma_M = 1.2$. The mean stiffness values consider the effect of load duration and humidity. Consequently, the adopted design values in both the direction of the fibers and perpendicular to the fibers are:

$$E_d = 1333.4\ N/mm^2$$

$$G_d = 150\ N/mm^2$$

$$f_{b,d} = 16.7\ N/mm^2$$

$$f_{t-c,d} = 8.3\ N/mm^2$$

$$f_{v,d} = 2.86\ N/mm^2$$

2.4. Loads acting on the structure

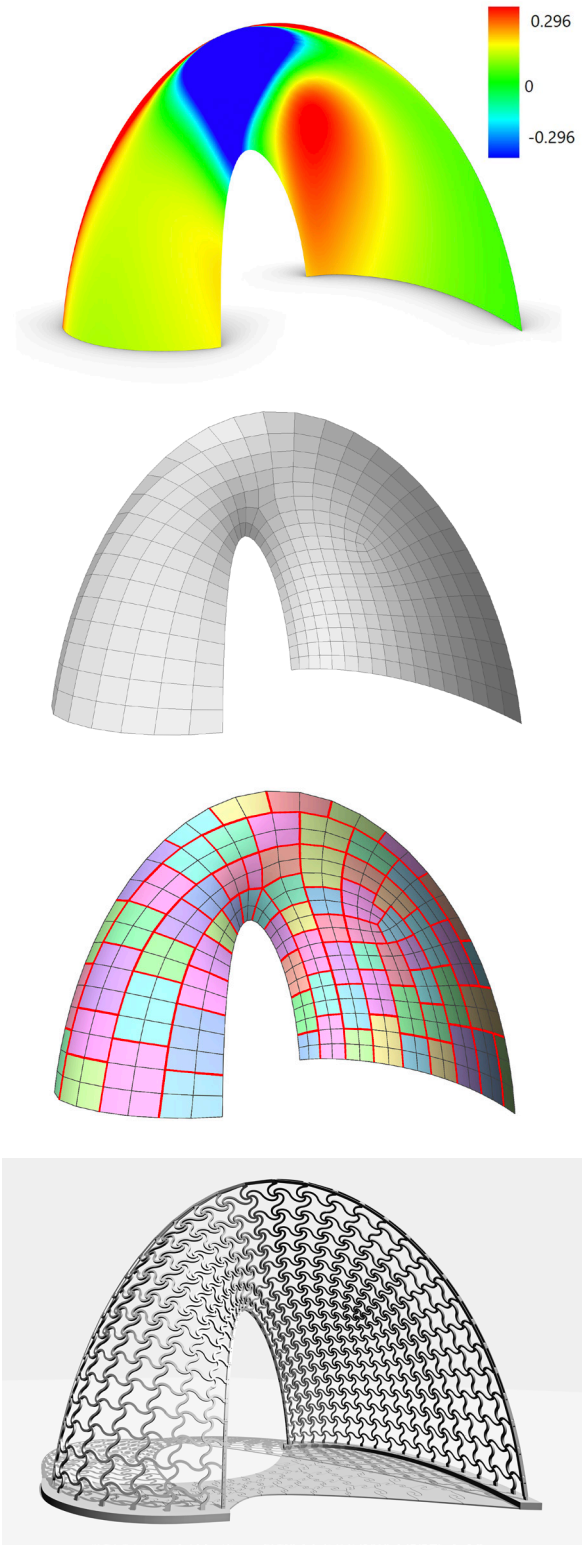

***Figure 6**: Computational design, from top to bottom: Gaussian curvature, quad mesh, patches, final design*

Applicable actions are taken into account according to EN 1991-1-1, EN 1991-1-3 and EN 1991-1-4. Moreover, these loadings are complying with EN 13782:2015, being the present structure a temporary installation. The main actions are permanent loads and pre-stress. The first ones are computed as characteristic value from the dead load due to self-weight. The second ones are deduced from the simulation of the bending of patches, which collects the story of deformation and stress from flat to their final configuration.

Variable actions are introduced as horizontal loads. The installation is not accessible to visitors, which can only walk around the structure without touching it nor walking through it nor on the supporting platform. For the sake of safety, a minimum amount of horizontal load is considered in the condition of environments without public access providing a value of $q_k = 0.30\ kN/m$ at the handrail height.

The stability is checked with a vertical uniformly distributed equivalent load of $q_{el} = 0.1\ kN/m^2$ on the outer surface of the shell. This load has not been combined with other load cases, except self-weight and pre-stress.

Since the structure is installed in an indoor environment, no other action is considered, i.e. wind forces, snow load, thermal actions. Seismic forces are not considered because of the flexibility and the lightweight nature of the structure. Finally, the structure is not designed to support general vertical live loading or construction loads.

The design values of the actions at the ultimate limit state (ULS) are deducted from the combinations EN 1990 and adopting national load combination factors (NTC18). For the serviceability limit state (SLS) the characteristic combination is considered (dead load and pre-stress included with unitary combination factors).

3. COMPUTATIONAL DESIGN

The computational design of FlexMaps structures relies on a displacement-based automated methodology [22-23], which can be summarized into three main steps: quad meshing, spirals' computation, and patching (Fig. 6).

In the meshing phase, the continuous shape is discretized into quad tiles that are constrained to be as regular as possible and to have approximately the same size. This process takes as input the dimension of the quad, which corresponds to the size of the spiral because each quad embeds a unique spiral. The endpoint of each spiral arm is on the edge's mid side. The adopted target quad edge size is $s = 0.25\ m$

(Fig. 7), and represents a compromise between fabrication feasibility and handling.

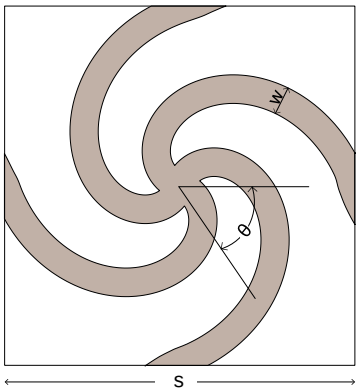

Figure 7: *Nomenclature of the spiral parameters (quad size s, width w, twist θ)*

Having thus fixed the first geometric parameter of the spiral, the actual computation optimizes for the other two variables, twist θ and width w, such that each spiral will have a specific stiffness to allow the overall shape reaching the target once assembled.

This problem is solved using a complex bounded optimization, where the displacements of the spirals are computed through an approximated beam model. For aesthetic reasons, the space of variables has been additionally limited to a constant width $w = 20\ mm$ and a twist range of $\theta = 100 - 250°$ (Fig. 7). The lower twist limit aims to avoid cross-like spirals. The upper has a further aim to avoid too dense spirals, whose arms may result too close with respect to the milling tolerance.

The patching step manages the positioning of the seams on the shape, namely selecting neighboring quads that can be grouped to form a patch, and is related to: a) developability, i.e. the capacity of a surface to be unrolled with low/no distortion; and b) fabricability, i.e. creating patches whose size makes them fabricable and easy to handle. On this later point, the IASS competition required all the components to fit into a maximum of six boxes up to 1.00x0.75x0.65 m and 32 kg each. Therefore, each patch is designed to group 2 up to 7 spirals for a total amount of 75 patches.

Based on their shape and size, the patches are nested into standard plywood sheets to be fabricated. However, as a result, the wooden fiber directions are randomly chosen since the nesting criterion is material saving.

4. STRUCTURAL ANALYSIS

The simplifications introduced in the computational design and the lack of information concerning stress have raised the need for a detailed structural analysis. The structure has been previously analyzed for the exposition at the IASS [25], and later the model has been detailed considering the more restrictive long-term installation at the Venice Biennale.

4.1. Finite element model

For the present case, a geometrically nonlinear solid model has been built and analyzed with the ANSYS package [26]. The model is generated with an automated workflow developed in conjunction with the algorithm employed for the computational design. The material model used in the analysis is linear elastic orthotropic, whose values are provided as per Sec. 2.3. The analysis is staged and consists of three consecutive load phases:

- *Pre-stress*. This load phase simulates the assembly of the patches made of 2 up to 7 spirals as they are individually bent and deformed to the target position. Each panel is initially arranged in the closest-possible position to its target deformed shape. This placement avoids large rigid displacements and improves the convergence of the analysis reducing the load steps. Then, a displacement is imposed at the extremities of the spirals' free arms to bring them in their deformed position. Consequently, the patch assumes its pre-stressed configuration.

- *SLS loading*. This phase follows the previous one and aims to simulate the actual behavior of the structure in operating conditions. In this phase, the patches extremes are coupled, and boundary conditions are applied. In this setup, the structure behaves as a whole. Bonding conditions are applied to couple the patches, and other boundary conditions are applied, i.e. fixed support to the ground and springs to model the edge beams. Gravity is applied.

- *ULS loading*. In this phase, several and different ULS combinations of loads are appended to the previous phase.

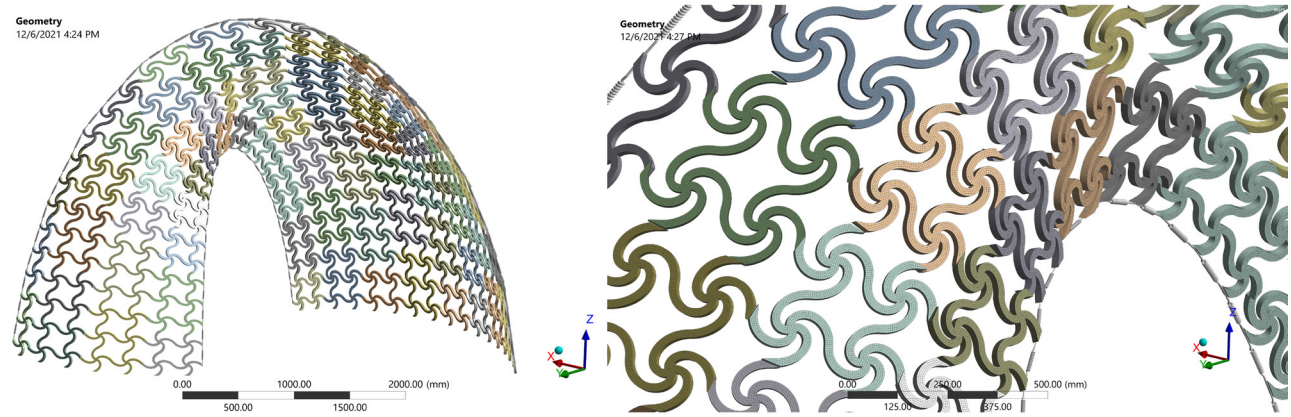

Figure 8: *FE model of the structure at the starting point before pre-stress (i.e. where the panels are not in contact but are floating in the flat configuration. The springs, the boundary conditions and the internal restraints are birth/death elements)*

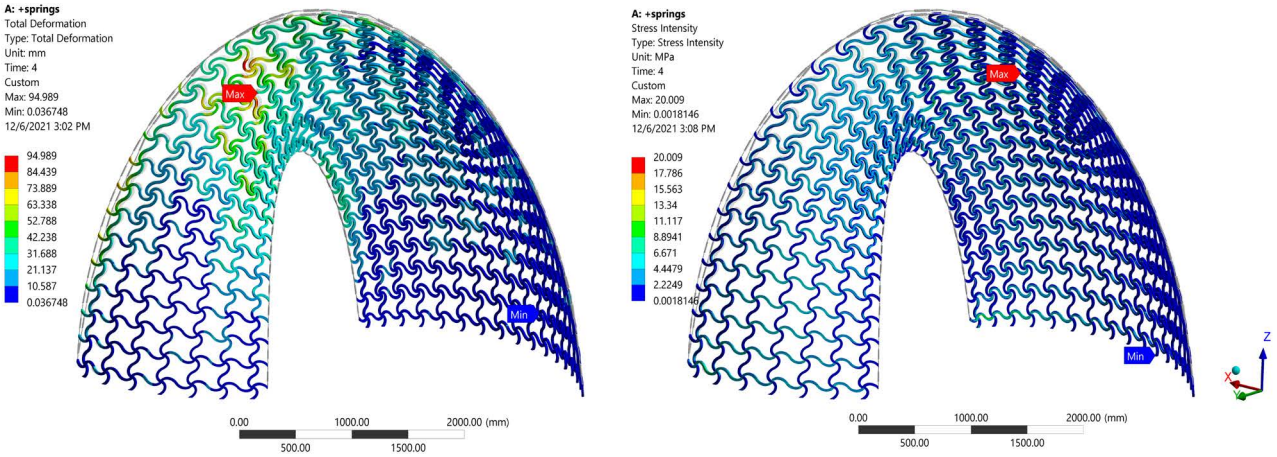

Figure 9: *SLS results: on the left, displacement; on the right, stress intensity.*

The structure is modeled as a 3D system made of 3D elements SOLID185 (Fig. 8). The material properties are applied to each patch according to the direction of the fibers deduced from the nesting. The meshing used in the FE analyses is generated from a NURBS solid model. The patch-to-patch joint is simplified as a face-to-face contact, whose elements are modeled through CONTA174 and are activated using birth/death capacity from phase 2 forward. This simplification appears to be reasonable in evaluating global performances of the structure and because the connection is designed to be stiff and resistant as the solid cross section.

The faces of the patches pointing to the ground are restrained from phase 2 forward with fixed boundary conditions. The edge beams are modeled as springs having only axial stiffness with a remote attaching on the boundary faces. These elements are activated from phase 2 forward as well. Although these lamellae are bending-active components, their stiffness due to pre-stress is neglected on the safe side.

The stability analysis is performed through an eigenvalue buckling analysis, using as starting point the results of a nonlinear analysis at ULS with q_{el}.

4.2. Analysis results

The accuracy of the whole method in matching a target shape can be quantified by evaluating the displacement change between Pre-stress phase, in which each spiral is forced to assume the target shape, and the SLS, in which these constraints are released. In Pre-stress phase, the spiral centers move in the range of 0-20 mm from their flat to target position. Then, at the SLS they move in the range of 0-40 mm (in absolute terms, i.e. with respect to the same flat position). Larger displacements are located in the center of structure where the spirals are softer

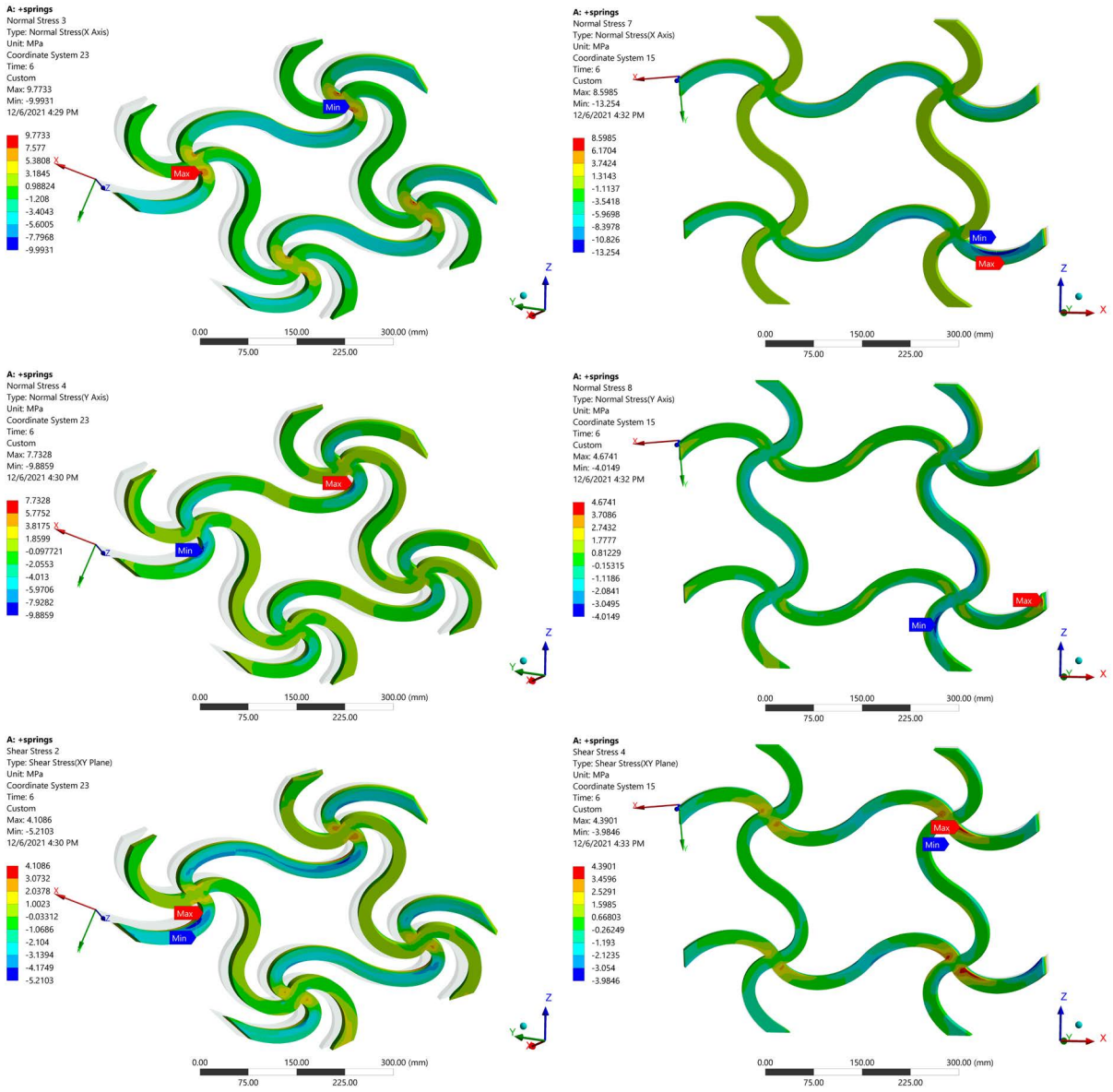

***Figure 10**: Patch 23 (left) and patch 15 (right) at ULS (with horizontal load): normal stress in X (top) and Y direction (middle), XY shear stress (bottom)*

by computational design to accommodate a larger curvature. The displacement values at the SLS are shown in Fig. 9 and represent a cumulative information that considers all the deformation history from the flat position to the SLS. Clearly the spiral arms accumulate more deformation due to pre-stressing than the center. Overall, the shape appears satisfactorily matched and the component elements well utilized as shown from the stress intensity map at the SLS in Fig. 9. The punctual strength verification is included in the next paragraph.

The modeling through brick elements allows to accurately check not only the deformations but also the strength by means of punctual verifications. Two of the most stressed patches are reported in Fig. 10. In general, the spiral is submitted to a complex stress state that includes bending, tension or compression, shear, and torsion. The verification is performed in the direction of the grain, perpendicular to the grain, and in shear, from which it can be stated that the patches have in general a sufficient residual capacity for the intended use. The analysis shows also peak values that are not considered because they are located at sharp features that are produced by localized modeling inaccuracies and simplifications, i.e. spiral arms merging at the center, patch-to-patch joint, and are drawbacks of the automatic generation of the FE model. Remarkably, the pre-stress phase as it is modeled here is more demanding than the ULS

in terms of stress, and as also confirmed by the experience it is the main source of failures.

The stability analysis of the structure results in a buckling multiplier of 1.83 (Fig. 11), which identifies a sufficient safety margin for such a temporary and indoor installation. This is significant considering that the structure is a lattice non-funicular shell, so it cannot rely on shape resistance. However, the eigenvalue buckling does not catch instability due to the progressive deformation that is associated with the in-plane softening of the spirals due to membrane action.

While the structure shows its best performances up to the SLS, from this point on, there are no stabilizing elements other than the edge and ground beams to prevent the occurrence of additional bending caused by further load. This is a limitation for the structure on developing the shell behavior, and it is further compounded by the adoption of a non-funicular target shape. Internally, the membrane action is moreover restricted by the spiral shaping, which mobilizes local bending of the arms in response to tension/compression forces. If compared with a patch of cross rods, a patch of spirals exhibits a non-symmetric and much softer behavior (Fig. 12). The higher is the spiral twist, the softer is the response and the smallest the ultimate load the patch can reach. The ultimate load is reached after large vertical displacement due to contact between the components, however the material strength limit is never attained. For this specific case in which the structure has only a showcasing purpose, the safety level is satisfactory. However, to better mobilize the membrane actions other measures have to be designed, especially for more demanding load bearing tasks.

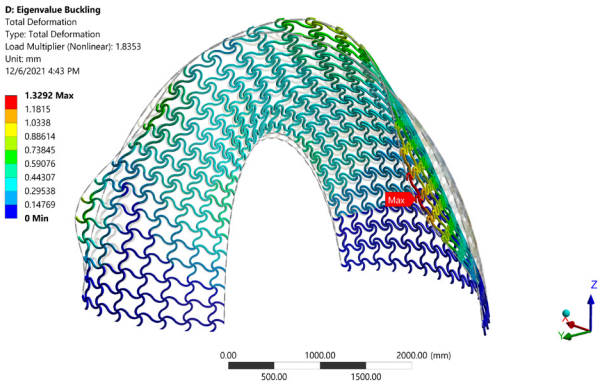

Figure 11: *Buckling shape for the load factor of 1.8353, eigenfrequency analysis*

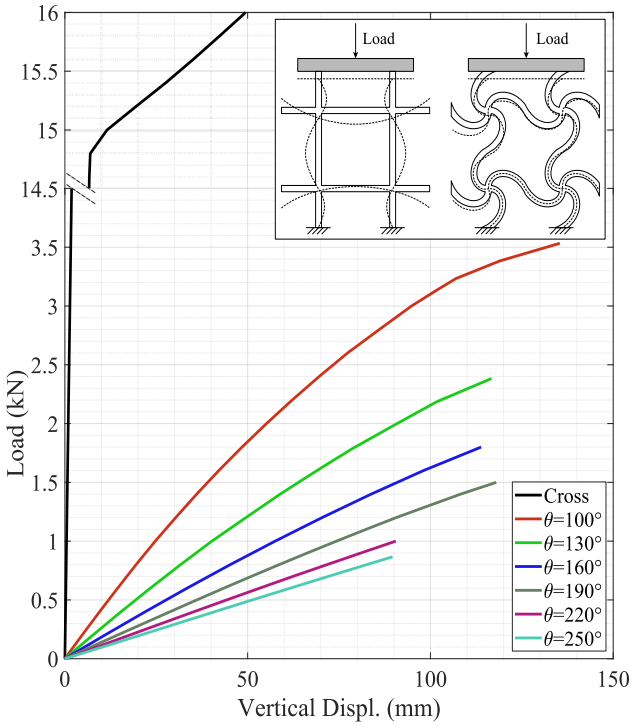

Figure 12*: Load-displacement plots for different patches in compression, compared with a standard patch made of cross elements. The patch is 0.5x0.5 m and uses the same structural properties adopted in the pavilion*

4.3. Connections

A local model is developed to assess the strength of the connection with respect to the ultimate capacity of the section forces provided by the incident spiral arms. The model is depicted in Fig. 13. The fiber direction is aligned with the X axis. The material adopted for bolts is common structural steel. The extremity face on the left is restrained for all displacement, while the following ultimate loads have been applied to the right face:

$F_x = \pm 3.32\ kN$
$F_y = 1.14\ \mathrm{kN}$

$F_z = 1.14\ \mathrm{kN}$

$M_y = \pm 22.27\ \mathrm{kN}mm$

$M_z = \pm 22.27\ \mathrm{kN}mm$

The results show that the connector is always over-resistant with respect to the spiral, and high stress that are beyond the material capacity are uniquely located in the transition zone from the 20 x 20 mm cross section of the spiral to the 25 x 25 mm of the connector or are localized peaks (Fig. 13).

The bolts worst case scenario occurs for F_z load, however the stress is well within the material

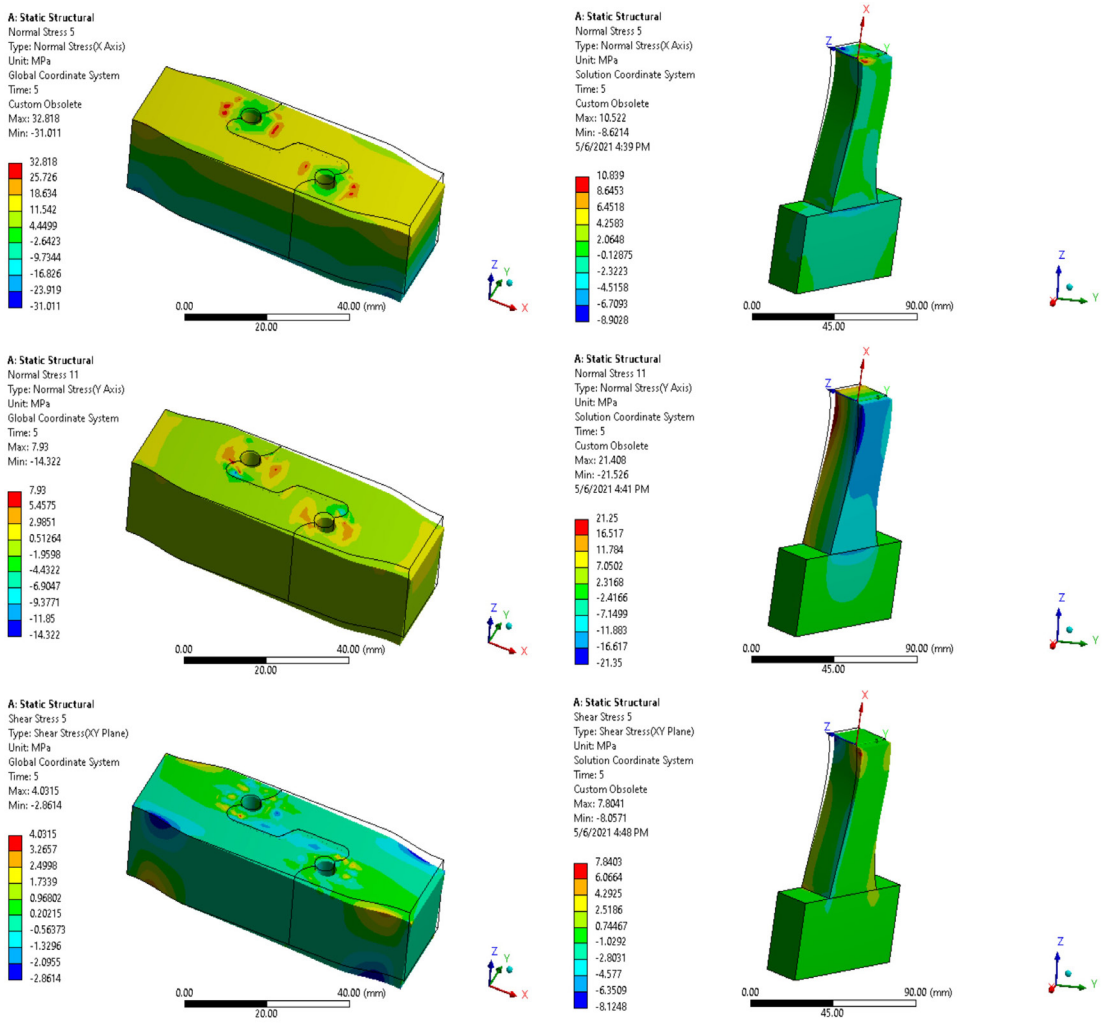

***Figure 13**: Patch-to-patch connection (left, bolts hidden) and T-footing (right), loaded by M_y: normal stress in X (top) and Y direction (middle), XY shear stress (bottom).*

capacity. Overall, the connector is safe and its performances can be considered satisfactory. The sliding and the lifting are safely avoided by screwing the ground profiles to the supporting platform. The overturning is inherently avoided due to the spatial arrangement of the system, however the anchoring provides redundancy to the connection. The system was already self-equilibrated in the IASS setup where only the paving provided sufficient balance to the supports forces.

The T-shaped footing loads are in the order of 100 times smaller than the full section capacity (Fig. 13). Therefore, the supports are able to safely support the design loads. Compression only restraints on the footing avoid translations in all directions.

5. CONSTRUCTION

5.1. Fabrication

The FlexMaps patches and components have been fabricated with a 3-axis milling machine starting from raw plywood panels of 1.5 x 3.0 m, 20 mm thick. In this subtractive fabrication process, the main information to provide to the machines is the elements' outline to distinctively identify tool paths (Fig. 14).

A CAM file is produced by assigning a specific tool and cutting speed for each path. In the present case, two settings have been selected for the interfaces of the patch-to-patch joint (3 mm diameter tool with 1.5 mm depth penetration) and the rest (6 mm diameter

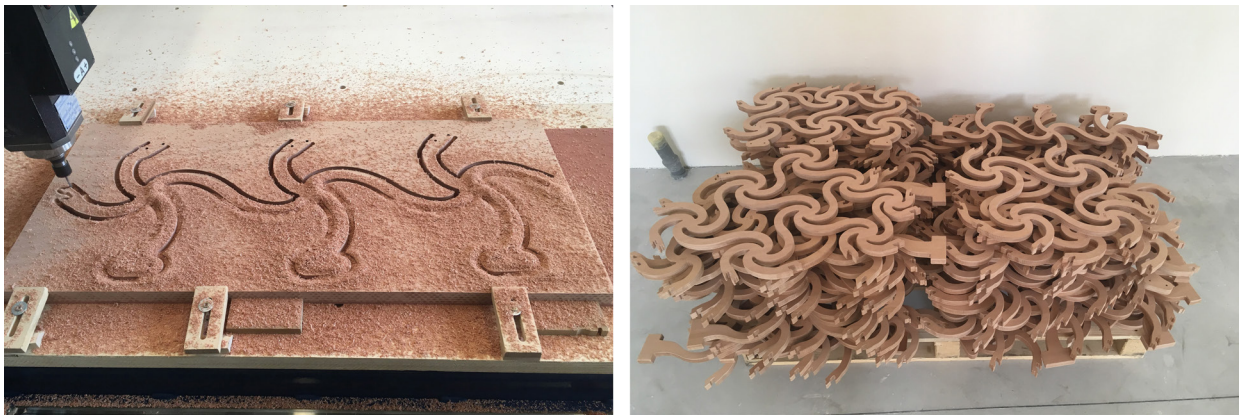

***Figure 14**: Fabrication of the FlexMaps patches*

***Figure 15:** Assembly of the FlexMaps Pavilion at the Biennale*

tool). The connectors have been previously tested to find a proper tolerance, which resulted in 0.13 mm on each side of the contour. A third tool setting has been used to carve a numeric label on each spiral to facilitate the assembly.

5.2. Assembly (and disassembly)

The Pavilion is assembled element by element going from the larger ground beam to the other. Each patch is sequentially bent and fastened to the neighboring ones. Accordingly, the structure gradually moves to the target global shape while gaining stiffness, as shown in Fig. 15. The edge beams play a fundamental role in this phase restraining the boundaries. Lastly, the structure is rigidly fixed on the supporting platform.

Conversely, to disassemble the structure it is necessary to release the restraint provided by the smaller edge beam in order to reduce the stiffness and disconnect all the elements one by one going backwards to the larger one.

All these steps are performed manually and are associated with several chances of failures (Fig. 16). Firstly, a major issue is represented by the exact sequence of assembly, which has not been pre-determined and has been referred to empirical evaluations. From the output of the FE simulation, the panels result resistant enough to be mounted but their assembly sequence is purely ideal. For that reason, to avoid failure, each element should be kept as close as possible to its final (assembled) position as any forced displacement may turn into breakage. To guarantee this condition and to avoid using a large temporary scaffolding and working at height, we tested as an effective procedure not to fix the first ground beam and allow rotation until almost all the patches are placed. Failure by traction or by bending (positive normal stress) as in Fig. 16a occurred when

(a) *(b)* *(c)*

***Figure 16**: Failure cases occurring during assembly/disassembly: (a) traction/bending; (b) delamination; (c) minor failures*

the patches were not connected sequentially, or they have been moved too far from their target position.

The patches are extremely easy to be jointed if they are not under stress, while the difficulty increases if they are bent. In both the assembly and disassembly, the friction between the interfaces of the connectors and the deformed configuration can lead to delamination as in Fig. 16b.

Except for limited cases (Fig. 16c), these failures are not reversible or negligible, and the component has to be replaced since a localized damage or restored parts constitute a stiffness alteration of the structure and could lead to a different equilibrium configuration. A limitation of such system, which is made of custom elements, is that failure can occur anywhere and there is no chance to rely on universal supply parts. Moreover, failures can be also triggered by material flaws.

6. VALIDATION AND MONITORING

The construction of the FlexMaps Pavilion as a large-scale demonstrator offered the opportunity to validate the design methodology. The real shape obtained through photogrammetry survey can be used for comparison with the FE results. Additionally, repeating the surveys in time can provide information on the evolution of the shape during the exhibition duration. Photogrammetry is a highly convenient technique as it requires only to take a set of photos of the object from different positions.

While photogrammetry could be able to densely reconstruct the whole geometry of the structure, due to the thinness of the spirals and the flat appearance of the surfaces, the resulting point cloud would probably be too noisy and scattered to be effectively compared with the CAD FE model. For this reason, we decided to track a specific set of points using markers.

In total, 48 markers (printed coded targets) have been affixed to both the base and the center of specific spirals all over the structure (Fig. 17). Since the base panels are fixed to the ground and will not move from one survey to the next, the 6 markers on the base act as Ground Control Points, to establish position, orientation, and scale of the photogrammetric surveys. The markers on the spirals are the points that will be measured and tracked across surveys.

The photogrammetric reconstruction is carried out in Agisoft Metashape [27]. The markers are automatically recognized by the software, and act as both "helpers" in the calibration/orientation of the photos (their location is used as a high-precision correspondence between input photos) and as "probes" (their position is determined in the reconstruction process).

The survey has been repeated three times, using the same setup of markers and a consistent set of photos (in terms of number of photos, general positioning, used camera and its parameters). The precision of the reconstructions does satisfy the requirements of the monitoring process. The residual error when matching the surveyed markers across the photos is below 1.8 pixels, while the residual error when fitting the Ground Control Points is below 1 mm.

At zero time (May 2021, after the assembly), the as-built structure presents a large misalignment from the FE deformed shape (Fig. 17), which is related to three main factors. Firstly, the ground beams relative

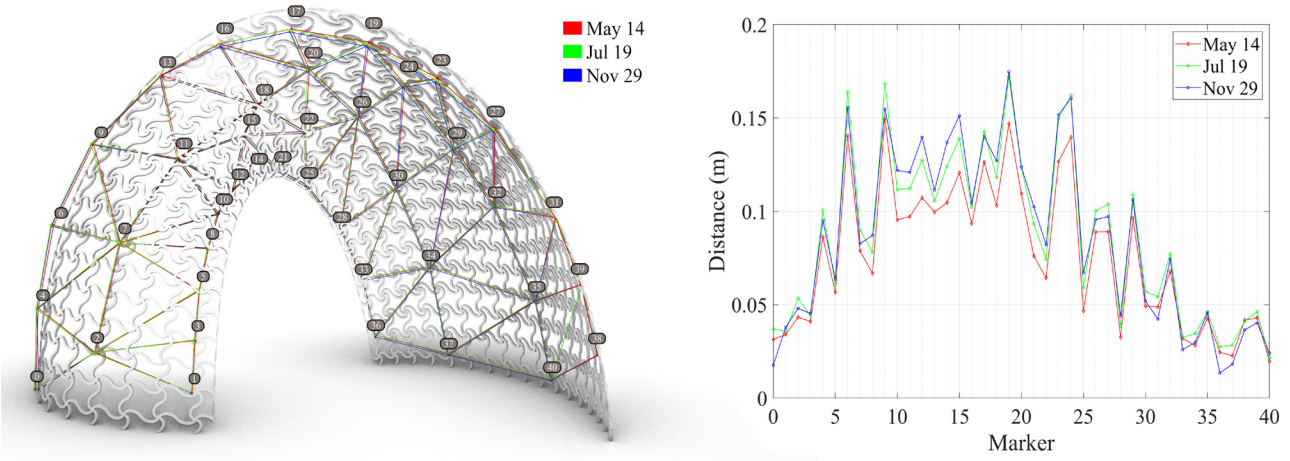

Figure 17: *Photogrammetry validation and monitoring: on the left, comparison of the expected FE deformed shape (solid model) with the actual surveyed shapes (colored, the graph connecting the points has only a visualization purpose); on the right, surveyed to expected distances at the markers*

distance has not been set accurately and it is larger than expected. Therefore, this error propagates, and the pre-stress of the patches is accordingly affected. Secondly, the accuracy of the shape depends uniquely on manual operations, on tolerances of the elements and on the guiding provided by the edge and ground beams. Therefore, a small error can unfavorably turn into large shape deviations. Thirdly, the edge beams' bending stiffness and pre-stress are not negligible in practice, and because of their constant cross section they push the inner and outer arch-shaped boundaries towards a rounded profile. Therefore, the as-built shape appears less pointed than expected. This deformation trend is not hindered by the expected displacement of the pavilion at the SLS (previous Fig. 9a).

This survey has been repeated to measure the effect of long-term exposure to humidity under constant load as it can accelerate the decrease of mechanical properties and long-term strength. Indeed, a shape softening is observed, and the displacement increases on average by 0.022 m in July 2021, and by 0.041 m in November 2021 (with respect to July).

From a visual check, the patches are not affected by breakages caused by long-terms effects. But, after disassembling the structure, they present a residual inelastic deformation as shown in Fig. 18 that prevents them from recovering the flat configuration. This result suggests that stiffness and strength are reduced and the chances of failure by material flaws are increased. Unfortunately, the limitations of the FE model make the quantification of the actual stiffness loss by reverse-fitting unfeasible.

7. CONCLUSIONS AND LIMITATIONS

The FlexMaps Pavilion has represented the first attempt to adopt bending-active mesostructures at the architectural scale and to monitor its behavior over a significant lapse of time. The shape of this structure has been selected with large design freedom, nonetheless its actualization reached a satisfying safety level as evidenced by the FE results and the verified behavior during the prolonged exposition at the Venice Biennale.

There are still open issues that should be considered to overcome the present limitations. In particular, the FE model strategy could be improved by considering properly the edge beams. In the assembly phase, a more effective base positioning or the introduction of some basic shape checks can positively affect the overall shape and behavior of the structure.

Regarding the structural behavior, improvements can be introduced to make this kind of structures definitively applicable for more general load-bearing purposes. By design, the spiral patches have a limited and highly variable membrane stiffness, which is convenient to reach the assembled configuration but could be not enough safe for a more considerable SLS load or other loading scenarios. Moreover, the shape design could not be completely unrestricted and shall consider the future behavior of the structure, i.e. being funicular. For instance, this is not applicable in the present case since the shape is not funicular, so as a lattice structure it will not have large stiffness for a larger SLS load, and any (undesired) further bending will be allowed.

Figure 18: *Inelastic deformation of patches after the Biennale exhibition*

On the material side, plywood has remarkable advantages from the fabrication point of view, but it introduces several problems as a layered anisotropic creep-sensitive material. From a stiffness perspective, the patch strength is affected by its positioning during the milling with respect to the base-material sheet orientation. From the material flaws perspective, the layers represent a weak spot for propagating failures and the narrow width of the spirals have the potential of increasing this effect (‘short grain effect’). Ultimately, as evidenced from the monitoring results, plywood softens when exposed to constant long-term loads and humid conditions, so evaluating different materials is recommended in the design phase of future FlexMaps structures.

ACKNOWLEDGMENTS

The FlexMaps Pavilion has been awarded First Prize at the “Competition and Exhibition of innovative lightweight structures” organized by the IASS Working Group 21 within the FORM and FORCE, joint international conference of IASS Symposium 2019 and Structural Membranes 2019 (Barcelona, 7-11 October 2019) with the following motivation: “for its structural innovation of bending-twisting system, connection constructability and exquisite craftmanship”[28].

The FlexMaps Pavilion has been exhibited at the 17th International Architecture Exhibition (22 May-21 November 2021), La Biennale di Venezia “How will we live together?” curated by Hashim Sarkis, Padiglione Italia “Resilient Communities” curated by Alessandro Melis, Vittorio Giorgini’s exhibition curated by Marco Del Francia [29].

The authors would like to acknowledge Bernd Bickel, Jesús Pérez, Emmanuel Iarussi, Eder Miguel; the Visual Computing Lab Staff of ISTI - CNR, in particular Massimiliano Corsini, Paolo Pingi; Antonio Rizzo of IPCF - CNR; the Administrative Staff of ISTI – CNR; and Antonio Chierici from our CNC service Manifattura Circolare.

REFERENCES

[1] N. Pietroni, D. Tonelli, E. Puppo, M. Froli, R. Scopigno, and P. Cignoni, "Statics aware grid shells, " *Computer Graphics Forum*, 34(2), pp. 627–41, 2015. (DOI: 10.1111/cgf.12590)

[2] C. Jiang, C. Tang, H-P Seidel and P. Wonka, "Design and volume optimization of space structures," *ACM Trans Graphics*, 36(4):159:1–159:14, 2017. (DOI: 10.1145/3072959.3073619)

[3] N. Pietroni, M. Tarini, A. Vaxman, D. Panozzo and P. Cignoni, "Position-based tensegrity design," *ACM Trans Graphics*, 36(6):172:1–172:14, 2017. (DOI: 10.1145/3130800.3130809)

[4] M. Kilian, D. Pellis, J. Wallner, and H. Pottmann, "Material-minimizing forms and structures, " *ACM Trans Graphics*, 36(6). (DOI: 10.1145/3130800.3130827)

[5] F. Gil-Ureta, N. Pietroni, and D. Zorin, "Reinforcement of general shell structures, " *ACM Trans Graphics*, 39(5). (DOI: 10.1145/3375677)

[6] F. Laccone, L. Malomo, M. Froli, P. Cignoni, and N. Pietroni, "Automatic Design of Cable-Tensioned Glass Shells, " *Computer Graphics Forum*, Vol. 39, No. 1, pp. 260-273, 2020. (DOI: 10.1111/cgf.13801)

[7] M. Popescu, L. Reiter, A. Liew, T. Van Mele, R.J. Flatt, and P. Block, "Building in concrete with an ultra-lightweight knitted stay-in-place formwork: prototype of a concrete shell bridge," *Structures*, Vol. 14, pp. 322-332, 2018. (DOI: 10.1016/j.istruc.2018.03.001)

[8] J. Brütting, J. Desruelle, G. Senatore, and C. Fivet, "Design of truss structures through reuse, " *Structures*, Vol. 18, pp. 128-137, 2019. (DOI: 10.1016/j.istruc.2018.11.006)

[9] C. Robeller, and N. Von Haaren, "Recycleshell: Wood-only Shell Structures Made From Cross-Laminated Timber (CLT)

Production Waste, " *Journal of the International Association for Shell and Spatial Structures*, 61(2), 125-139, 2020. (DOI: 10.20898/j.iass.2020.204.045)

[10] B. Bickel, P. Cignoni, L. Malomo, N. Pietroni, "State of the art on stylized fabrication," *Computer Graphics Forum*, 37(6):325–342, 2018. (DOI:10.1111/cgf.13327)

[11] X. Yu, J. Zhou, H. Liang, Z. Jiang, and L. Wu, "Mechanical metamaterials associated with stiffness, rigidity and compressibility: A brief review," *Progress in Materials Science*, 94:114–173, 2018. (DOI: 10.1016/j.pmatsci.2017.12.003)

[12] J. Lienhard, H. Alpermann, C. Gengnagel, and J. Knippers, "Active bending, a review on structures where bending is used as a self-formation process, " *Int J Space Struct* , 28 (3–4) pp.187–96, 2013. (DOI: 10.1260/0266-3511.28.3-4.187)

[13] C. Gengnagel, E.L. Hernández, and R. B¨aumer, "Natural-fibre-reinforced plastics in actively bent structures," *Proc Inst Civil Eng-Constr Mater*, 166(6):365–77, 2013. (DOI: 10.1680/coma.12.00026)

[14] P. Nicholas, and M. Tamke, "Computational strategies for the architectural design of bending active structures," *Int J Space Struct*, 28(3–4), pp. 215–28, 2013. (DOI: 10.1260/0266-3511.28.3-4.215)

[15] J. Lienhard, *Bending-active structures: form-finding strategies using elastic deformation in static and kinetic systems and the structural potentials therein*, 36, Institut für Tragkonstruktionen und Konstruktives Entwerfen (ITKE). Universit¨at Stuttgart 2014. (DOI: 10.18419/opus-107)

[16] J. Lienhard, and J. Knippers, "Bending-active textile hybrids," *J Int Assoc Shell Spatial Struct*, 56(1), pp. 37–48, 2015. ISSN 1028-365X.

[17] D. Sonntag, S. Bechert, and J. Knippers, "Biomimetic timber shells made of bending-active segments," *Int J Space Struct*, 32 (3–4):149–59, 2017. (DOI: 10.1177/0266351117746266)

[18] M. Tamke, Y.S. Baranovskaya, F. Monteiro, J. Lienhard, R. La Magna, M.R. Thomsen. "Computational knit – design and fabrication systems for textile structures with customised and graded CNC knitted fabrics," *Architect Eng Design Manage*, 1–21, 2020. (DOI: 10.1080/17452007.2020.1747174)

[19] N. Kotelnikova-Weiler, C. Douthe, E.L. Hernandez, O. Baverel, C. Gengnagel, and J.F. Caron, "Materials for actively-bent structures," *Int J Space Struct*, 28(3–4), pp. 229–40, 2013. (DOI: 10.1260/0266-3511.28.3-4.229)

[20] R. La Magna *Bending-active plates: strategies for the induction of curvature through the means of elastic bending of plate-based structures*, 43, Institut für Tragkonstruktionen und Konstruktives Entwerfen (ITKE). Universit¨at Stuttgart 2017. (DOI: 10.18419/opus-9389)

[21] J. Panetta, M. Konakovi´c-Lukovi´c, F. Isvoranu, E. Bouleau, M. Pauly, "X-shells: a new class of deployable beam structures," *ACM Trans Graphics* 38(4). (DOI: 10.1145/3306346.3323040)

[22] L. Malomo, J. Pérez, E. Iarussi, N. Pietroni, E. Miguel, P. Cignoni, and B. Bickel, "FlexMaps: computational design of flat flexible shells for shaping 3D objects," *ACM Trans Graphics*, 241, 2018. (DOI: 10.1145/3272127.3275076)

[23] F. Laccone, L. Malomo, N. Pietroni, P. Cignoni, and T. Schork, "Integrated computational framework for the design and fabrication of bending-active structures made from flat sheet material," *Structures*, Vol. 34, pp. 979-994, 2021. (DOI: 10.1016/j.istruc.2021.08.004)

[24] F. Laccone, L. Malomo, J. Pérez, N. Pietroni, F. Ponchio, B. Bickel, and P. Cignoni, "FlexMaps Pavilion: a twisted arc made of mesostructured flat flexible panels," in *Proceedings of IASS Annual Symposia* (Vol. 2019, No. 5, pp. 1-7). International Association for Shell and Spatial Structures (IASS). (2019, October)

[25] F. Laccone, L. Malomo, J. Pérez, N. Pietroni, F. Ponchio, B. Bickel, and P. Cignoni "A bending-active twisted-arch plywood structure: computational design and fabrication of the FlexMaps Pavilion," *SN*

Applied Sciences, 2(9), pp. 1-9, 2020. (DOI: 10.1007/s42452-020-03305-w)

[26] ANSYS. Academic Research Mechanical Release 18.0.; 2018.

[27] AgiSoft Metashape Professional (Software). (2021). Retrieved from http://www.agisoft.com/downloads/installer/

[28] IASS Working Group 21 (organizers),"Competition and Exhibition of innovative lightweight structures", at the FORM and FORCE, joint international conference of IASS Symposium 2019 and Structural Membranes 2019 (Barcelona, 7-11 October 2019): https ://www.jjo33 .com/iass-barcelona-2019

[29] A. Melis, B. Medas, T. Pievani, *Catalogo del Padiglione Italia «Comunità Resilienti» alla Biennale Architettura 2021. Catalogo della mostra* (Vol. 1/b), D Editore, ISBN 8894830683